Title

The hydration of bentonite buffer material revealed by modeling analysis of a long-term in situ test

Authors

Zheng, Liange
Xu, Hao
Rutqvist, Jonny
et al.

Publication Date

2020-02-01

DOI

10.1016/j.clay.2019.105360

Peer reviewed

The hydration of bentonite buffer material revealed by modeling analysis of a long-term *in situ* test

Liange Zheng[1]*, Hao Xu[1], Jonny Rutqvist[1], Matthew Reagan[1], Jens Birkholzer[1], María Victoria Villar[2], Ana María Fernández[2]

[1*]Lawrence Berkeley National Laboratory, lzheng@lbl.gov

[2]Centro de Investigaciones Energéticas Medioambientales y Tecnológicas, Madrid, Spain

Abstract

The hydration of a bentonite barrier in the early stage of a geologic nuclear waste repository with a bentonite buffer is a critical issue for its long-term performance and safety because bentonite might be permanently altered and subsequently affect the function of bentonite barrier. Large scale *in situ* testing integrated with modeling analysis is an effective way to study the key processes affecting the hydration of a bentonite barrier. In this paper, through the comparison between coupled thermal, hydrological, mechanical, and chemical (THMC) models and data from a long term *in situ* test, we attempt to pinpoint the importance of non-Darcian flow, thermal osmosis, and hydro-mechanical coupling (porosity and permeability change due to swelling) to the hydration rate of the bentonite barrier under heating conditions.

We found that a TH model equipped with non-Darcian flow severely underestimates the relative humidity and water content measured in the bentonite. Calibration of the parameters associated with relative permeability overshadows the contribution of non-Darcian flow, and non-Darcian flow under unsaturated conditions is not yet fully understood. An empirical relationship between saturated permeability and dry density was found to work better than a saturated permeability that is the function of effective stress in matching the relative humidity, water content data, and the chloride concentration in pore water. We also found that chemical data are actually helpful in

calibrating the THM model. A question regarding the relevance of thermal osmosis to the hydration process, in terms of matching models and data, remains unanswered. Although a THMC model with thermal osmosis matches all THMC data nicely, similar goodness-of-fit can also be achieved by a THMC model without thermal osmosis but with lower permeability. We learned that the robustness of the model could be increased if the model is tested against long-term data and multiple types of data, and given that non-uniqueness is inevitable, more independent measurements of key parameters and multi-scale and multi-physics tests may help approximate the right model for evaluating the safety of the repository.

1. Introduction

Deep geological disposal of radioactive waste typically involves a repository with multiple barriers. In addition to the natural barrier system, i.e. the host rock and its surrounding subsurface environment, the repository also has an engineered barrier system (EBS). The EBS represents the man-made, engineered materials placed within a repository, including the waste form, waste canisters, buffer materials, backfill, and seals.

The most commonly proposed buffer material for EBS is compacted bentonite, which features low permeability, high swelling capacity and strong retardation of radionuclide transport. Initially, the emplaced bentonite is partially saturated with dry density typically ranging from 1.4 to 1.7 g/cm^3. Over time, the bentonite buffer should become fully saturated by water infiltration from the host rock through a complicated process involving multiphase flow, heating from the waste packages, evaporation/condensation, and more importantly, porosity/permeability changes over the course of hydration. The hydration of bentonite in the early stage may have profound impact the on long-term properties of bentonite barrier, such as the permeability and stability of bentonite. This might affect the safety functions of the EBS, which include limiting transport in

47 the near field, limiting pressure on the canister, supporting excavation walls, and reducing
48 microbial activity. The bentonite hydration phase coincides with the early time high temperature
49 period of the repository, which might result in irreversible changes of bentonite that affect the
50 ability of bentonite retarding the migration of radionuclides. It is therefore critical to have a
51 thorough understanding of the processes that control the hydration of the bentonite buffer and
52 have models that are capable of describing these processes reliably.
53 Hydration of unsaturated bentonite has been extensively studied by experiments and models for
54 laboratory column tests (e.g Börgesson et al., 2001; Åkesson et al., 2009; Chijimatsu et al., 2009;
55 Tong et al., 2010; Graupner et al., 2018) and field tests (Kanno et al., 1999; Rutqvist et al., 2001)
56 at all kinds of scales (e.g. Lloret and Villar 2007; Villar et al., 2018) and different model
57 approaches. While coupled thermal, hydrological and mechanical (THM) models with
58 multiphase Darcy flow have typically been used to simulate the hydration of bentonite (e.g. Gens
59 et al., 1998; Rutqvist et al., 2001; Hökmark, 2004; Chen et al., 2009; Sánchez et al., 2012a),
60 other approaches, such as the extended vapor diffusion model (Kröhn, 2019), have been
61 investigated as well. Integration of modeling and large-scale field experiments is an effective
62 way of understanding the hydration of bentonite barrier. The FEBEX (**F**ull-scale **E**ngineered
63 **B**arrier **Ex**periment in crystalline host rock) project performed *in situ* and mock-up tests,
64 numerous small-scale laboratory tests, and thermal, hydrological and chemical (THC) and THM
65 modeling (ENRESA, 2000), and has greatly improved the understanding of bentonite hydration.
66 When modeling the water infiltration into the bentonite in mock-up tests (e.g. ENRESA, 2000;
67 Zheng et al., 2008) and small scale heating and hydration tests (Zheng et al., 2010), TH models
68 that consider heat transport and Darcy-type multiphase flow were not able to match the data—

neither the spatial distribution of water content at end of the test (Zheng et al., 2010), nor the temporal evolution of water influx data (Zheng and Samper, 2008). Porosity/permeability changes due to the swelling of bentonite upon hydration must be included in the model. THM models were mostly used to analyze these tests. A fairly large number of models have been developed for the small scale FEBEX tests (Zheng et al., 2010), mock-up tests (Sánchez et al., 2005; Zheng and Samper, 2008; Sánchez et al., 2012b), and the *in situ* test at early stages (Alonso et al., 2005; Nguyen et al., 2005; Chen et al., 2009), intermediate stages (Gens et al., 2009; Zheng et al., 2011; Sánchez et al., 2012a), and final stages (Samper et al., 2018). When reviewing the FEBEX *in situ* and mock-up tests after 15 years of operation, Lanyon and Gaus (2016) concluded that the second order processes, namely coupled processes such as thermal osmosis, and porosity structure evolution were controlling the hydration of the bentonite in addition to the first order processes (flow driven by hydraulic gradients). When the models for FEBEX *in situ* and mock-up test were examined, these models have features in common: hydration of bentonite was one of a series of coupled processes, the TH model was not sufficient to explain the data, and coupled THM processes were needed to simulate the hydration of bentonite. However, these models also differ in details, including whether thermal osmosis is relevant, what kind of mechanical models could/should be used, e.g. state surface approach (Nguyen et al., 2005) or Barcelona Expansive Model (Sánchez et al., 2012a)), and how permeability changes are related to porosity. Box and Draper's comments (Box and Draper, 1987) on statistical modeling, "all models are wrong, but some are useful," might also be applied to the THM models for bentonite. But it seems unquestionable that models that survived the test of more data, e.g. longer history of temporal data and more temporal snapshots of spatial data are more useful. When the FEBEX *in situ* test was dismantled and comprehensive THMC data were

available, a simple TH model was developed and the level of complexity was gradually increased until a coupled THMC model was achieved. The purpose of the modeling work in this paper is to test the relevance of certain coupled processes to bentonite hydration and to pinpoint the constitutive relationships for coupled processes, or less ambitiously, learn what THMC modeling can/cannot do to delineate processes. This paper starts with a very brief description of the test, presents the model and data, and then discusses the processes that are likely relevant or irrelevant to the hydration of bentonite.

2. A brief description of FEBEX *in situ* experiment

The FEBEX *in situ* test was conducted at the Grimsel underground laboratory, Switzerland (ENRESA, 2006). It consisted of five basic components: the drift, the heating system, the bentonite barrier, the instrumentation, and the monitoring and control system. The main elements of the heating system were two heaters (#1 and #2), 1 m apart. Heaters were placed inside a cylindrical steel liner and were at constant-temperature control mode to maintain a maximum temperature of 100ºC at the steel liner/bentonite interface 61 days after the heating started. The bentonite barrier was made of blocks of highly compacted bentonite. The initial dry density and the water content of compacted bentonite blocks were 1.7 g/cm^3 and 14%, respectively. If gaps between blocks and at areas near the rock wall and steel liner were considered, the average dry density of entire bentonite barrier was around 1.6 g/cm^3.

The *in situ* test began on February 27, 1997 and went through two dismantling events (see Table 1 for the operation timeline). A comprehensive post-mortem bentonite sampling and analysis program was performed during both dismantling events (Bárcena et al., 2003; Garcia-Sineriz et al., 2016).

In the FEBEX *in situ* test, some data were collected by the sensors installed in the bentonite, such as temperature, relative humidity and stress; and some of them were measured in the laboratory using the bentonite samples that were taken after dismantling of test sections, including water content and dry density. The dismantling of heater #1 in 2002 and heater #2 in 2015 (Table 1) provided two snapshots of measured water content, dry density, and ion concentrations in the pore water of the bentonite, which are very valuable for understanding the temporal evolution of these key data. In this paper, in addition to THM data, measured chloride concentration is the only chemical data that were used to constrain models.

3. Model development

The model interpretation of the FEBEX *in situ* test started from a simple TH model and gradually increased the level of complexity until a coupled THMC model was developed that could match all of the THMC data.

3.1 Simulator

The numerical simulations were conducted with TOUGHREACT-FLAC3D (Zheng et al., 2015a; 2017), which sequentially couples the multiphase fluid flow and reactive transport simulator, TOUGHREACT V3.0-OMP (Xu et al., 2014), with the finite volume geo-mechanical code FLAC3D (Itasca, 2009). A recent addition to the code is the capability of simulating non-Darcian flow (Zheng et al. 2015b) and thermal osmosis.

3.2 The conceptual model

In the current model, both conductive (Fourier's law) and convective heat flux are considered. The model considers non-isothermal two-phase (air and water) flow, with individual phase fluxes given by a multiphase version of Darcy's Law. For the vapor flow in the air phase, in addition to Darcy flow, mass transport can also occur by diffusion and dispersion according to Fick's law.

The mechanical process was controlled by the momentum balance equation with a state-surface approach to describe the constitutive relationship between stress and pore pressure. The solute transport was described by advection-dispersion equation. The general energy balance equation and the mass balance equations for multiphase flow are given in the manual of TOUGH2 code (Pruess et al., 1999); the details of solving transport and chemical reactions are given in Xu et al. (2014). Coupling between THMC processes was done through constiitutive relationships. Some obvious and important couplings implemented in the code are TC (the effect of temperature on chemical reactions), HC (the effect of transport on chemical reactions), TM (the effect of temperature on mechanical deformation and stress), and HM (the effect of fluid pressure on mechanical deformation and stress) couplings. In this paper, TH coupling, including saturation-dependent thermal conductivity (Eq. (1)) and thermal osmosis (Eq. (4)) and HM coupling via density-dependent permeability (Eq. (3)) were of particular interest.

Because over the span of water saturation that FEBEX bentonite went through (from an initial degree of water saturation 55-59% to 100%), the thermal conductivity/water saturation relationship can sufficiently be represented by a linear relationship; we use a linear relationship implemented in TOUGH2 (Pruess et al., 1999):

$$\lambda_h = \lambda_{wet} + S_l\left(\lambda_{wet} + \lambda_{dry}\right) \quad (1)$$

where λ_{wet} is the thermal conductivity under fully saturated conditions, λ_{dry} is the thermal conductivity under dry conditions, and S_l is the liquid saturation degree. λ_{wet} and λ_{dry} are given in Table 2. Although measured thermal conductivity versus saturation were properly represented with sigmoidal type relationship (ENRESA, 2000), the linear relationship used in the current model and other model (Kuhlman and Gaus, 2014) led to a sufficient match between the measured temperature and model results, because over the range of water saturation that FEBEX

159 bentonite went through, model results were not sensitive to the type of relationship (linear vs
160 sigmoidal type relationship).
161 Table 2 lists the thermal and hydrological parameters. Key parameters affecting the hydration of
162 bentonite were the permeability of granite, the relative permeability and retention curves of
163 bentonite, the vapor diffusion coefficient, and the permeability and thermo-osmotic permeability
164 of bentonite, all calibrated based on current modeling work. The rest of parameters were
165 measured for FEBEX bentonite (ENRESA, 2006).
166 Granite is a fractured medium and should ideally be represented by a multi-continuum method
167 with both fracture and matrix properties. As in previous models for the *in situ* test (Alonso et al.,
168 2005; Samper et al., 2008; Sánchez et al., 2012a), the current model assumes granite is a
169 homogeneous porous medium, which requires the use of an equivalent effective permeability. A
170 permeability of 2×10^{-18} m^2 was used (Table 2) based on model calibration, which was within in
171 the range of plausible values (7×10^{-19} to 8×10^{-18} m^2) according to the granite permeability
172 measured in the field (ENRESA, 2006) and calibrated in other models (Zheng et al., 2011;
173 Sánchez et al., 2012b; Kuhlman and Gaus, 2014).
174 The capillary pressure (retention curve) was represented by the van Genuchten function (van
175 Genuchten, 1980) :
176

$$P_{cap}=\frac{-1}{\alpha}\left(\left[s^{¿}\right]^{-1/m}-1\right)^{1-m} \qquad (2)$$

177
178 where P_{cap} is the capillary pressure (Pa), $s^{¿}=(s_l-s_{lr})/(1-s_{lr})$ and S_l is the water saturation, S_{lr} is
179 the residual water saturation. S_{lr} is 0.1 for bentonite and 0.01 for granite. The values of α and m

180 are given in Table 2. The retention curve was fairly well studied for FEBEX bentonite, with a
181 variation of m from 0.18 to 0.6 (ENRESA, 2006; Zheng et al., 2011; Sánchez et al., 2012b;
182 Kuhlman and Gaus, 2014).
183 The effective permeability of bentonite has been under scrutiny by modelers (e.g. Zheng et al.,
184 2011) due to its critical role in determining the hydration of bentonite. It is the product of
185 intrinsic permeability (k) (or saturated permeability/absolute permeability) and relative
186 permeability (k_r). Relative permeability using $k_r=S_l^3$ (where S_l is water saturation degree) has
187 been consistently used by different models (Zheng et al., 2011; Sánchez et al., 2012b; Kuhlman
188 and Gaus, 2014) and the same function was used here. The plausible intrinsic permeability for
189 FEBEX bentonite in the initial state could range from 1×10^{-21} to 9×10^{-21} m^2 based on various
190 sources (ENRESA, 2000; Zheng et al., 2011; Sánchez et al., 2012b; Kuhlman and Gaus, 2014;
191 Chen et al., 2009) and 2.15×10^{-21} m^2 was used in the model. However, as demonstrated by Zheng
192 et al. (2015b), a constant intrinsic permeability for bentonite could not explain the relative
193 humidity data over the entire thickness of the bentonite barrier.
194 The stress-dependence of permeability for low-permeability sedimentary rock is fairly well
195 known and has been studied extensively (e.g. Kwon et al., 2001; Ghabezloo et al., 2009). Many
196 empirical relationships have been put forward to describe the permeability changes with effective
197 stress. Eventually, an empirical relationship modified from the permeability-dry density
198 relationship derived in Villar (2002) was used:

$$logk=(-2.96\rho_d-8.57)/\alpha \qquad 3$$

199 where ρ_d is dry density. A scaling factor, α of 1.882, was added to the original permeability-dry
200 density relationship (ENRESA, 2000) such that initial permeability is 2.15×10^{-21} m^2 .

According to coupled transport phenomena, thermal, hydraulic, and chemical gradients all have effects on the heat, liquid, and solute fluxes. The direct and coupled phenomena for different transport processes can be described by the Onsager matrix (Table 3).

Thermal osmosis is a coupled process that can produce a fluid flux. Zhou et al. (1999) showed that additional coupled flow terms due to a temperature gradient had significant effects on the distribution of capillary pressure and saturation degree in a THM model of a thick cylinder heating test. The flux of fluid caused by thermal osmosis v_{to} can be written as (Dirksen, 1969):

$$v_{to} = -k_T \nabla T \quad (4)$$

where T is temperature and k_T is the thermo-osmotic permeability ($m^2/K/s$). Liquid flux caused by thermal osmosis term can be added to Darcian terms (Ghassemi and Diek, 2002; Zhou et al., 1999). In current model, k_T of 1.2×10^{-12} $m^2/K/s$ is used.

In Zheng et al. (2016), two mechanical models for bentonite were tested: a linear swelling model and the dual structure Barcelona expansive clay model (BExM), and the result was that both models led to similar fits to measured THM data. Both methods had pros and cons: BExM provided a sophisticated description of the swelling of bentonite, but it is more computationally expensive and contains a large number of parameters difficult to calibrate, whereas linear swelling models had a simple parameterization with a few parameters that could be easily calibrated (though it does not describe correctly the transient state of swelling). Eventually, for the THMC model for the FEBEX *in situ* test, a method that is somewhat in between was used: the state surface approach.

To consider the nonlinear elastic behavior, the poro-elastic coefficients of the equation are expressed as functions of suction (s) and net stress ($\sigma_m^{''}$) by adopting the concept of a state surface equation (Matyas and Radhakrishna, 1968). Based on results of oedometric tests, Lloret and Alonso (1985) proposed the equation of void ratio on the state surface:

$$e = A + B\ln\left(-\sigma_m^{''}\right) + C\ln\left(s + p_a\right) + D\ln\left(-\sigma_m^{''}\right)\ln\left(s + p_a\right) \quad (5)$$

where e is the void ratio; p_a is atmospheric pressure; A, B, C and D are empirical constants;

$\sigma_m^{''} = \left(\frac{\sigma_{kk}}{3}\right) - p_g$ is the mean net stress and $s = p - p_g$ is the suction, where p_g is the gas pressure. In this case, A, B, C, and D are the only material parameters needed to calibrate for the model on the specific material. For the FEBEX compacted bentonite, these parameters are equal to A = 0.805, B = - 0.07524, C = - 0.057, and D = 0.00479977. Rutqvist and Tsang (2003) and Nguyen et al. (2005) used the same approach to simulate the THM behavior during the first three years of the FEBEX *in situ* test, but the values for the empirical constants in Eq. (5) calibrated in current model were slightly different because the models assumed different initial capillary pressure.

The chemical model only includes the advection and dispersion of chloride. The final calibrated effective diffusion coefficient for Cl was the $\varnothing^{1/3} S^{10/3} \times 2 \times 10^{-10} m^2/s$ where $\varnothing$ is porosity and S is water saturation. Depending on time and location, the effective diffusion coefficient ranged from 8×10^{-14} m^2/s to 1.4×10^{-12} m^2/s, with effective diffusion coefficient for most time and locations around 0.4—1.4×10^{-12} m^2/s. There is growing consensus that the anion is excluded from some pore space, the so-called "anion exclusion." If we use Bradbury and Baeyens (2003) pore-space concept, chloride will presumably only migrate in macro-pores, but not in the micro-pores. However, the current model assumes all the pores are available for the transport of

chloride for two reasons: one is that the pore space concept for the chemical model has to be consistent with that of flow and mechanical models, which do not distinguish macro and micro-pores, and the other is the consistency with the measured data. The chloride concentration in the pore water was measured by the aqueous extract (Sacchi et al., 2001), a method to quantify the total content of soluble salts of a clay sample. An *1:R* aqueous extract test consisted of adding to a mass M_s of clay sample a mass of distilled water equal to R times M_s. Clay sample and water were stirred during a period of time of usually 2 days during which equilibration of water and clay sample was allowed. Chemical analyses were performed on supernatant solution after phase separation by centrifugation (Sacchi *et al.*, 2001). Dilution happens during aqueous extract preparation, and chloride concentrations had to be corrected to the water content of the clay sample before adding distilled water (this was referred as "calibrated chloride concentration" later when results were presented). Because water content is a macroscopic quantity and cannot reflect different levels of pores, the correction was made with reference to the entire pore volume. Subsequently, to be comparable with chloride data, the model assumed that the entire pores were available for chloride transport. The initial concentration of chloride was 0.16 mol/-kg water (Fernández et al., 2001) in bentonite pore water and 1.3×10^{-5} mol/kg water in granite water (ENRESA, 2000).

3.3 Modeling setup

Because axi-symmetrical (Villar et al., 2018), an axi-symmetrical mesh was used (Fig. 1) to save computation time and focus on the key coupling processes. However, such a model can only be used to interpret and predict the THMC behavior in the "hot sections", i.e. sections of bentonite blocks surrounding the heater.

The model considers two material zones: one for the bentonite and the other for the granite. The wall of the canister (r = 0.47 m) is located at the interface between node 1 and 2, node 1 (centroid coordinate at r=0.468) and has the properties of the canister, and node 2 (centroid coordinate at r=0.471) has the properties of bentonite. The simulation time started on February 27, 1997 and ended on July 1, 2015, a total of 6,698 days (18.3 years).

The initial temperature was uniform and equal to 12ºC. A constant temperature of 100ºC was prescribed at the heater/bentonite interface (r = 0.47 m), while the temperature was assumed to remain constant at its initial value of 12ºC at the external boundary (r = 50 m) because the thermal perturbation induced by the heaters over the time frame of the experiment did not extend to this distance. The bentonite had an initial gravimetric water content of 14%, which corresponds to a saturation degree of 55% and a suction of 1.11×10^2 MPa. Because the current model does not consider the gaps between bentonite, heater and rock wall, the initial dry density of bentonite was assumed to be 1.63 g/cm^3.The boundary conditions for flow included: 1) no flow at r = 0.47 m and 2) a prescribed liquid pressure of 0.7 MPa at r = 50 m based on the hydrological characterization of the granite drift (ENRESA, 2000). Initial total stress was 0.15 MPa in bentonite, which led to an initial effective stress of 0.05MPa. Initial total stress in granite ranged from 0.15 MPa to 11.5 MPa in the host rock depending on the radial distance. Zero normal displacement was prescribed at r = 0.47 m and 50 m. Note that the model is axi-symmetric and one-dimensional, and thus does not have vertical or horizontal stress. After the bentonite filled the drift, the radial/circumferential stress was dependent on the distance from the boundary confinement.

4. Processes controlling the hydration of bentonite revealed by model results and data

The data available for the FEBEX *in situ* test include temporal evolution of temperature and relative humidity as measured by sensors installed in the bentonite at radial distances of around 0.5 m (close to the heater), 0.8 m, and 1.05 m (close to the granite), as well as stress data collected by sensors at radial distances around 0.5 m and 1.1 m. Characterization after dismantling of heater #1 in 2002 (5.3 years from the start of the test) and heater #2 in 2015 (18.3 years from the start of the test) provided two snapshots of measured water content, dry density, and chloride concentration (Villar et al., 2016; Fernández et al., 2018). Model results at some times and locations are not sensitive to changing parameters and processes, for example, temporal temperature evolution at radial distance of 0.5 and 0.8 m and temporal relative humidity evolution at radial distance of 1.05 m (which are not shown in the paper), and data at these times and locations can be matched by basically any models and therefore we are unable to delineate better models through goodness-of-fit between model results and data. Some data are challenging for models to match, and are shown here to illustrate why complex models are needed. These include temporal evolution of relative humidity at radial distance of 0.5 m in section E1 and E2 (ENRESA, 2006), water content measured at 5.3 years from section 19, 28, and 29 (see Figure 4.39 in ENRESA (2006) for locations of the sections) and 18.3 years from section 49 (Villar et al., 2016). Temperature data at radial distance of 1.05 m in section E2 and F2 (ENRESA, 2006) and stress at radial distance 1.1 m from sections E2 and F2 ((ENRESA, 2006) are also presented for completeness. Chloride concentration data at 5.3 years from section 19, 28, and 29 (Zheng et al., 2011) were calibrated from data measured by aqueous extract (Fernández and Rivas, 2003); chloride concentration data at 18.3 years from section 53 were

307 calibrated from data measured by aqueous extract in Fernández et al.(2018). All data were
308 collected from "hot" sections, i.e. sections of bentonite blocks surrounding the heater.
309 A series of TH/THMC models were conducted and compared (Table 4) to facilitate the
310 evaluation of processes that might be important to the hydration of bentonite and the goodness-
311 of-fit between data and these simulations was employed as the criteria for delineation of the
312 importance or relevance of these processes.

313 **4.1 Non-Darcian flow**

314 As aforementioned, the threshold gradient for flow (i.e. non-Darcian flow) within bentonite was
315 identified as one of the second-order processes that may be relevant (Lanyon and Gaus, 2016).
316 Therefore, non-Darcian flow was added to the TH model, aiming to resolve the discrepancy
317 between model and relative humidity data to some extent, while acknowledging that non-Darcian
318 flow may likely not solve all the problems as other processes might also be at play, especially
319 HM couplings.

The general form of non-Darcian flow was developed in Liu and Birkholzer (2012). The key of having non-Darcian flow model was reliable calculation of the threshold gradient. Based on data from various sources, the threshold gradient I and permeability k (m^2) have the following relationship (Liu and Birkholzer, 2012):

$$I = A\,k^{B} \tag{6}$$

320 with A= 2.0×10^{-13} and B = -0.78 calibrated based on a permeability test for FEBEX bentonite
321 (Samper et al., 2008b).
322 After implementing non-Darcian flow into the simulator according to Liu and Birkholzer (2012),
323 a non-Darcian flow TH model was developed for the FEBEX *in situ* test. The non-Darcian flow

models significantly underestimated the measured relative humidity data (Fig. 2), even in bentonite near the bentonite/granite interface (radial distance around 1.05 m).

The relevance of non-Darcian behaviour is clear for saturated flow in clay rock (Liu and Birkholzer, 2012 and references cited therein) and intuitively one would think that non-Darcian behaviour should also be relevant to unsaturated flow in clay rock. However, when the numerical model was used to evaluate such relevance, there are issues that might prevent us from clearly delineating the contribution of non-Darcian flow to unsaturated clay or bentonite. First and foremost, the calibration of the relative permeability and retention curves overshadows the effect of non-Darcian flow. The non-linear relationship between water flux and hydraulic gradient, which motivates the relevance of non-Darcian behavior to water flow, is already accounted for, at least partially, by the relative permeability (which in turn is a function of the retention curve) in the flux-gradient relationship for unsaturated flow. In other words, the non-linear relationship between water flux and hydraulic gradient for unsaturated flow might be affected by two features: non-Darcian flow and relative permeability. However, in most modeling exercises, relative permeability is calibrated based on a Darcy-type flow. As a result, the calibration of the parameters associated with relative permeability overshadows the contribution of non-Darcian flow— the parameters for relative permeability might be "over-calibrated" so that the effect of non-Darcian flow looks irrelevant. For FEBEX bentonite, the relative permeability and retention curve were calibrated based on a Darcy-type flow model (ENRESA, 2000), which essentially obviates non-Darcian flow for unsaturated bentonite. Thus, if non-Darcian flow is added on top of relative permeability that is calibrated based on Darcy flow, as in the model presented in this section, the non-linearity between flux and gradient are double-counted, and consequently the model would significantly underestimate the water inflow from granite to bentonite, as shown in

Fig. 2. This is essentially an issue of process uncertainty versus parameter uncertainty, which is faced by many complex models. Second, Cui et al. (2008) reported that threshold gradients were different for different capillary pressures. In this paper, we used the equation proposed by Liu and Birkholzer (2012) in which threshold gradient is solely a function of saturated permeability. Further research is needed to take into account the effect of capillary pressure when a threshold gradient is calculated. However, even though the threshold gradient calculation can be improved by taking into account capillary pressure, it would unlikely eliminate the issue of process uncertainties versus parameter uncertainties.

4.2 The base THMC model

Because TH model overestimated the relative humidity data (Fig. 2), water content data (Fig. 4 and 5), additional processes were added seeking better match between data and model. First, mechanical effects, using the state surface approach (Eq. (5)) were added to the model to simulate the swelling of bentonite, expanding the model from a TH to a THM model. As a result of the swelling, the porosity changed, as did the permeability. A variable permeability as function of dry density (Eq. (3)) was used. Second, another coupled process, thermal osmosis, was added to the model, using a calibrated thermal osmotic permeability. Finally, the transport of chloride was added to THM model to form a THMC model. Note that in the current model, the THM processes affect the chemical process, but not vice-versa because the chemical process only involves the transport of chloride, not mineral precipitation/dissolution. Even if mineral precipitation/dissolution was considered in the model (e.g. Zheng et al., 2016), the porosity change due to minerals phase alteration would be very small and subsequently the chemical process would have little effect on the THM processes.

The calibrated THMC model, referred to as the base THMC model in this paper, was able to provide a reasonable match to the measured temporal evolution of temperature (Fig. 3) , relative humidity (Fig. 2), and measured spatial distribution of water content at 5.3 (Fig. 4) and 18.3 years (Fig. 5), stress at several radial distances (Fig. 6), and the chloride concentrations measured at 5.3 years (Fig. 7) and 18.3 years (Fig. 8). This confirmed the necessity of using a THM model to explain the hydrological behavior of bentonite. However, TH and THMC models led to similar temperature profiles, as exemplified by Fig. 3, indicating it was not necessary to use a full THM/THMC model to calculate temperature evolution. The TH model overestimated significantly the water content data at 18.3 years, but only slightly at 5.3 years, signifying the importance of having long-term data for calibration.

As shown in Table 1, there was a cooling period between the shutdown of the heaters and the beginning of bentonite sampling: 103 days after heater #1 was dismantled and 70 days after heater #2 was dismantled. The water-content data obtained immediately after dismantling represent the moisture distribution after the cooling period. Fig. 4 shows the modeled water content at 5 years (right before cooling period) and 5.3 years (after cooling period) during the dismantling of heater #1; and Fig. 5 shows modeled water content at 18.1 and 18.3 years, before and after the cooling period during the dismantling of heater #2. The model results showed significant moisture re-distribution—water content near the heater rose significantly, while water content from the middle of the barrier to granite decreased slightly. Thus, models need to consider the cooling period to account for the water content profile properly.

4.3 The permeability functions

The permeability function is unquestionable very important for the hydration of bentonite. In the current model, permeability was represented as function of dry density (Eq. (3)). Other forms of permeability functions have been published, for example, the exponential law (David et al., 1994):

$$k = k_0 \exp[-\gamma(\sigma - \sigma_0)] \quad (7)$$

where k is the permeability at the effective stress σ, k_0 is the permeability at initial stress σ_0 and is equal to 2.15×10^{-21} m^2; γ is the stress sensitivity coefficient and equal to 1×10^{-7} Pa^{-1} based on previous models (Zheng et al., 2016). The stress-dependence of permeability for low-permeability sedimentary rocks is fairly well known and has been studied extensively (e.g. Kwon et al., 2001; Ghabezloo et al., 2009). Many empirical relationships have been put forward to describe the permeability changes with effective stress. Eq. (7) is just one of them. In order to evaluate the effect of different permeability function on the hydration of bentonite, we conducted a simulation that used Eq. (7) for the permeability evolution while other processes and parameters remained the same as base THMC model (Run A). Run A led to faster hydration of bentonite than in the base THMC model, which was clear in the temporal evolution of relative humidity (Fig. 2). Run A produced a temperature evolution slightly different from the base THMC model (Fig. 3) because the different water saturation profile in Run A and the base THMC model led to slightly different thermal conductivities according Eq. (1). The stresses calculated by Run A and the base THMC model were very similar and fell into the range of stress data (Fig. 6). Examining just temperature, stress, and water content data, it is hard to conclude that the base THMC model outperformed Run A. The underperformance of Run A in matching data was rather clear in the temporal evolution of relative humidity (Fig. 2) and

411 concentration profile of Cl (Fig. 7 and 8). Run A was not able to match the Cl data at 5.3 and
412 18.3 years, likely due to the different computed effective permeability profiles in the base THMC
413 model and in Run A (Fig. 9). In the base THMC model, high permeability in the area close to
414 granite led to higher dilution and subsequently lower Cl concentration therein. In the middle of
415 the barrier, permeability was relatively low, which led to lesser degree of dilution and higher Cl
416 concentrations , which matched the data well. In contrast, in Run A, permeability at the area near
417 the granite and the middle of barrier were roughly the same, which led to too much dilution in
418 the middle of barrier, and thus the simulation did not match the chloride data.
419 Both relative humidity and chloride concentration data helped to differentiate the base THMC
420 model and Run A, but temperature, stress and water content data did not. It is intuitively
421 understandable that hydrological data, i.e. relative humidity, would help to evaluate hydrological
422 parameters, i.e. permeability function in this case. However, it is less obvious that chemical data,
423 i.e. chloride concentration in this case, can actually be helpful in discerning the validity of
424 hydrological parameters. If relative humidity data were not available, without chloride
425 concentration data, the base THMC model and Run A are indistinguishable in matching the
426 temperature, stress and water content data. The lessons learned here are that chemical data can
427 provide an additional piece of information for calibrating a THM model, and it is important to
428 have a variety of data to determine the best model and the correct model parameters.

429 **4.4 The relevance of thermal osmosis**

430 Although thermal osmosis was included in the current THMC model and some previous models
431 (Zheng at al., 2011, Samper et al., 2018), some THM models that did not consider thermal
432 osmosis matched reasonably well the THM data in the *in situ* test (e.g. Gens et al., 2009;
433 Sánchez et al., 2012a). The question raised here is whether thermal osmosis is relevant to the

hydration of bentonite under heating conditions, and whether the data available are capable of evaluating its relevance. This question could be answered by performing an additional simulation disabling thermal osmosis and adjusting parameters.

Run B is a simulation similar to the base THMC model in Section 4.2, but not including thermal osmosis. The temporal evolution of relative humidity at locations near the heater (see Fig. 2) in Run B was higher than that in the base case after 4.5 years. The spatial profile of water content at 18.3 years was higher than that in the base case in the area within radial distance < 0.8 m (Fig. 5) despite the fact that the water content profile at 5.3 years in Run B was very similar to that in the base THMC model (Fig. 4). Run B and the base THMC model had a very similar Cl concentration profile at 5.3 years (Fig. 7), but differed moderately at 18.3 years (Fig. 8). Relative humidity and water content data and results at later times point out that removing thermal osmosis from the model led to faster hydration of bentonite and discrepancies between the data and the model.

In terms of hydration of bentonite, thermal osmosis is essentially slowing down the hydration from the granite by creating a moisture flux in the direction opposite the water infiltration from the granite. The question is whether the same temporal relative humidity evolution and spatial water content profile could be achieved by changing other parameters that affect water transport in bentonite—those parameters have uncertainties as well. In the current model, the vapor diffusion coefficient and intrinsic permeability have significant impact on the water movement in bentonite, therefore two additional runs were conducted: Run C, which was similar to Run B, but had a higher effective vapor diffusion coefficient (2×10^{-4} m^2/s, almost 3 times higher than that in the base THMC model) and Run D, which was similar to Run B, but had lower initial intrinsic permeability (1.5×10^{-21} m^2/s vs 2.15×10^{-21} m^2/s in the base THMC model).

Compared to the base THMC model, Run C had no thermal osmosis but higher vapor diffusion to see if thermal osmosis retarded the water infiltration effectively the same way as high vapor diffusive flux. Base THMC model and Run C had rather similar temporal evolution of relative humidity (Fig. 2), water content (Fig. 4) and Cl concentration profile (Fig. 7) at 5.3 years. However, discrepancy between base THMC model and Run C was observed for the water content (Fig. 5) and Cl concentration (Fig. 8) at 18.3 years; Results from Run C were not able to match the water content data and Cl concentration at 18.3 years as close as the base THMC model, which illustrates the importance of having data for longer time period.

A comparison between the base THMC model and Run D (no thermal osmosis, but lower permeability) confirmed that the decrease in hydration rate by thermal osmosis was effectively the same as by reducing permeability, as Run D and the base THMC model have very similar results for temporal evolution of relative humidity (Fig. 2) and water content profiles at 5.3 years (Fig. 4) and 18.3 years (Fig. 5), and the evolution of Cl concentration profiles at 5.3 years (Fig. 7) and 18.3 years (Fig. 8). The similarity between Run D and base THMC model explained why some models (e.g. Sánchez et al., 2012a) can also match THM data without considering thermal osmosis. It seems that, from the point of matching data from the *in situ* test with coupled THMC model, we cannot determine whether thermal osmosis is relevant to the hyration of bentonite under heating conditions. Based on the coupled flow theory, thermal osmosis should be considered in the THMC model for the bentonite barrier. However, the effect of thermal osmosis could easily be overshadowed by using lower permeability which is well within the uncertainty range of the data.

5. Discussion and conclusion

While laboratory tests and corresponding models are helpful for understanding key processes and parameters regarding the hydration of bentonite barrier, ultimately large-scale *in situ* tests integrated with models have to be used to study the key safety issues related to the bentonite barrier. In this paper, coupled THMC models for a long term FEBEX *in situ* test for bentonite barrier were presented, in an attempt to shed light on key processes that control the hydration of the bentonite barrier under heating conditions.

Knowing that a TH model with Darcy flow using constant porosity and permeability is incapable of matching data, a TH model equipped with non-Darcian flow was conducted to improve the goodness-of-fit, but this model severely underestimated the hydrological data. The fact that the non-Darcian flow seems irrelevant may be because the calibration of the parameters associated with relative permeability overshadows the contribution of Non-Darcian flow, and that non-Darcian flow under unsaturated condition is not fully understood.

Eventually, a THMC model that considers two-phase flow, changes in porosity and permeability due to mechanical processes, and thermal osmosis is shown to match the data available from the *in situ* test: namely temporal evolution of temperature, stress, relative humidity at several radial distances, and the spatial distribution of water content and Cl concentration at two times. While the relevance of vapor diffusion and the change in porosity due to swelling and hydration leaves is undisputed, how to describe the change of permeability and the relevance of thermal osmosis is still under debate. Sensitivity runs were therefore conducted to answer these two questions.

The base THMC model resorted to an empirical relationship between permeability and dry density which was measured specifically for FEBEX bentonite. Using a more common empirical relationship for permeability, an exponential law in which permeability is the function of

effective stress, produced less satisfactory results in terms of matching long-term water content data and Cl concentration—chemical data are actually helpful to calibrate the THM model. However, the current model cannot rule out the possibility that other empirical relationship might lead to similar results (which is quite likely).

The question regarding the relevance of thermal osmosis to the hydration process, solely from the point of view of matching data to the model, remains unanswered. A sensitivity run without thermal osmosis but with lower permeability produced very similar THMC results to the base THMC model (with thermal osmosis) and matches the data equally well as the base THMC model. In general, regarding developing and calibrating coupled THMC models, the lessons learned are:

(1) Robustness of model can be increased if the model is tested against long-term data and various types of data. Short-term data and the use of single data points may fail to reveal the deficiency of the model.

(2) Given the complexity of coupled THMC model, non-uniqueness is inevitable—different models can reach similar goodness-of-fit for the same data set. Because of that, the current model and data are unable to determine the relevance of thermal osmosis.

Ultimately multi-scale experiments and models, more accurate measurement of key parameters, and additional data will help us to develop a model that can evaluate the safety of the repository.

Acknowledgments

Funding for this work was provided by the Spent Fuel and Waste Science and Technology, Office of Nuclear Energy, of the U.S. Department of Energy under Contract Number DE-AC02-05CH11231 with Lawrence Berkeley National Laboratory. Data from the test site were provided through FEBEX-DP consortia.

524

525 **Reference**

526 Åkesson, M., Jacinto, A.C., Gatabin, C., Sanchez, M., Ledesma, A., 2009. Bentonite THM
527 behaviour at high temperatures: experimental and numerical analysis. Géotechnique
528 59(4), 307-318.
529 Alonso, E.E., Alcoverro, J., Coste, F., Malinsky, L., Merrien Soukatchoff, V., Kadiri, I., Nowak,
530 T., Shao H., Nguyen, T.S., Selvadurai, A.P.S., Armand, G., Sobolik, S.R., Itamura, C.M.,
531 Stone, C.M., Webb, S.W., Rejeb, A., Tijani, M., Maouche, Z., Kobayashi, A., Kurikami,
532 H., Ito, A., Sugita, Y., Chijimatsu, M., Börgesson, L., Hernelind, J., Rutqvist, J., Tsang,
533 C.F., Jussila, P., 2005. The FEBEX Bechmark test. Case Definition and comparison of
534 modelling approaches. International Journal of Rock Mechanics and Mining Sciences,
535 42, 611-638.
536 Bárcena, I., Fuentes-Cantillana, J.L., García-Siñeriz, J.L., 2003. Dismantling of the Heater 1 at
537 the FEBEX "in situ" test. Description of operations. Enresa Technical Report 9/2003.
538 Börgesson, L., Chijimatsu, M., Nguyen, T.S., Rutqvist, J., Jing, L., 2001. Thermo-hydro-
539 mechanical characterization of a bentonite-based buffer material by laboratory tests and
540 numerical back analyses. International Journal of Rock Mechanics and Mining Sciences,
541 38, 105-127.
542 Kanno, T., Fujita, T., Takeuchi, S., Ishikawa, H., Hara, K., Nakano, M., 1999. Coupled thermo-
543 hydro-mechanical modelling of bentonite buffer material. International Journal for
544 Numerical and Analytical Methods in Geomechanics 23(12), 1281-1307.
545 Box, G.E.P., Draper, N.R., 1987. Empirical Model-Building and Response Surfaces. John Wiley
546 & Sons.
547 Bradbury, M.H., Baeyens, B., 2003. Porewater chemistry in compacted re-saturated MX-80
548 bentonite. Journal of Contaminant Hydrology, 61(1–4), 329-338.
549 Ghabezloo, S, Sulem, J, Guédon, S, Martineau, F. 2009. Effective stress law for the permeability
550 of a limestone. Int. J. Rock Mech. Min. Sci. 46:297-306.
551 Chen, Y., Zhou, C., Jing, L., 2009. Modeling coupled THM processes of geological porous
552 media with multiphase flow: Theory and validation against laboratory and field scale
553 experiments. Computers and Geotechnics, 36(8), 1308-1329.
554 Chijimatsu, M., Börgesson, L., Fujita, T., Jussila, P., Nguyen, S., Rutqvist, J., Jing, L., 2009.
555 Model development and calibration for the coupled thermal, hydraulic and mechanical
556 phenomena of the bentonite. Environmental Geology 57(6), 1255-1261.
557 Cui, Y.J., Tang, A.M., Loiseau, C., Delage, P., 2008. Determining the unsaturated hydraulic
558 conductivity of a compacted sand-bentonite mixture under constant-volume and free-
559 swell conditions. Physics and Chemistry of the Earth 33, S462-S471
560 David, C,Wong, T.F, Zhu, W., Zhang, J., 1994 Laboratory measurement of compaction- induced
561 permeability change in porous rocks: implications for the generation and maintenance of
562 pore pressure excess in the crust. Pure Appl Geophys. 143, 425–456.
563 Dirksen, D., 1969. Thermo-osmosis through compacted saturated clay membranes. Soil Sci. Soc.
564 Am. Proc., 33(6), 821-826.
565 ENRESA, 2000. Full-scale engineered barriers experiment for a deep geological repository in
566 crystalline host rock FEBEX Project. EUR 19147 EN, European Commission.

ENRESA, 2006. Full-scale engineered barriers experiment updated final report 1994-2004. ENRESA technical publication 05-0/2006, P590.

Fernández, A.M., Cuevas, J., Rivas, P., 2001. Pore water chemistry of the FEBEX bentonite. Mat. Res. Soc. Symp. Proc. 603, 573-588.

Fernández, A.M., Sánchez-Ledesma, D.M., Melón, A., Robredo, L.M., Rey, J.J., Labajo, M., Clavero, M.A., Carretero, S., González, A.E., 2018. Thermo-hydro-geochemical behaviour of a Spanish bentonite after of the FEBEX in situ test at the Grimsel Test Site.Technical report CIEMAT/DMA/2G216/03/16. NAB16-025. Madrid, 256 pp.

Garcia-Sineriz, J.L., Abós, H., Martínez, V., De la Rosa, C., Mäder, U., Kober, F., 2016. FEBEX-DP Dismantling of the heater 2 at the FEBEX "in situ" test. Nagra Arbeitsbericht NAB 16-011. p. 92

Ghabezloo S, Sulem J, Guédon S, Martineau F. Effective stress law for the permeability of a limestone. International Journal of Rock Mechanics and Mining Sciences. 2009;46:297-306.

Gens, A., Garcia-Molina, A.J., Olivella, S., Alonso, E.E., Huertas, F., 1998. Analysis of a full scale in situ test simulating repository conditions. International Journal for Numerical and Analytical Methods in Geomechanics 22(7), 515-548.

Gens, A., Sánchez, M., Guimarães, L. D. N., Alonso, E. E., Lloret, A., Olivella, S., Villar, M. V., and Huertas, F., 2009. A full-scale in situ heating test for high-level nuclear waste disposal: observations, analysis and interpretation. Géotechnique, 59(4): 377-399.

Ghassemi, A. Diek, A., 2002. Porothermoelasticity for swelling shales. Journal of Petroleum Science and Engineering, 34, 123-125.

Graupner, B.J., Shao, H., Wang, X.R., Nguyen, T.S., Li, Z., Rutqvist, J., Chen, F., Birkholzer, J., Wang, W., Kolditz, O., Pan, P.Z., Feng, X.T., Lee, C., Maekawa, K., Stothoff, S., Manepally, C., Dasgupta, B., Ofoegbu, G., Fedors, R., Barnichon, J.D., E. Ballarini, E., Bauer, S., Garitte, B., 2018. Comparative modelling of the coupled thermal-hydraulic-mechanical (THM) processes in a heated bentonite pellet column with hydration. Environmental Earth Sciences 77:84. https://doi.org/10.1007/s12665-018-7255-3

Horseman S.T., McEwen, T.J., 1996. Thermal constrains on disposal of heat-emitting waste in argillaceous rocks, Engineering Geology 41, 5-16.

Hökmark, H. 2004. Hydration of the bentonite buffer in a KBS-3 repository. Applied Clay Science 26(1–4): 219-233.

Itasca, 2009. FLAC3D, Fast Lagrangian Analysis of Continua in 3 Dimensions, Version 4.0, Minneapolis, Minnesota, Itasca Consulting Group.

Kanno, T., Fujita, T., Takeuchi, S., Ishikawa, H., Hara, K., and Nakano, M., 1999. Coupled thermo-hydro-mechanical modelling of bentonite buffer material, In International Journal for Numerical and Analytical Methods in Geomechanics, pp 1281-1307.

Kuhlman, U., Gaus, I., 2014. THM Model validation modelling of selected WP2 experiments: Inverse Modelling of the FEBEX in situ test using iTOUGH2. DELIVERABLE-N°: D3.3-1, NAGRA.

Kröhn, K.P., 2019. Re-saturation of compacted bentonite under repository-relevant flow conditions. Geomechanics for Energy and the Environment 17: 115-122.

Kwon, O., Kronenberg, A.K., Gangi, A.F., Johnson, B., 2001, Permeability of Wilcox shale and its effective pressure law. J. Geophys. Res.-Sol. Ea.,106, 19339-53.

611 Lanyon, G.W., Gaus, I., 2016. Main outcomes and review of the FEBEX In Situ Test (GTS) and
612 Mock-up after 15 years of operation, Technical Report 15-04, Nagra,
613 Liu, H.H., Birkholzer, J., 2012. On the relationship between water flux and hydraulic gradient for
614 unsaturated and saturated clay. Journal of Hydrology 475: 242-247.
615 Lloret, A, Alonso, E.E., 1985. State surfaces for partially saturated soils. Proceedings of the
616 International Conference on Soils Mechanics and Foundation Engineering, vol. 2.
617 Balkema, 557–62.
618 Lloret, A. and Villar M. V. 2007 "Advances on the knowledge of the thermo-hydro-mechanical
619 behaviour of heavily compacted “FEBEX” bentonite." Physics and Chemistry of the
620 Earth, Parts A/B/C 32(8–14): 701-715.
621 Matyas, E.L., Radhakrishna, H.S., 1968. Volume change characteristics of partially saturated
622 soils. Geotechnique, 30(4), 432–48.
623 Nguyen, T.S., Selvadurai, A.P.S., Armand, G., 2005. Modelling the FEBEX THM experiment
624 using a state surface approach. International Journal of Rock Mechanics and Mining
625 Science, 42(5-6), 639-651.
626 Pruess, K., Oldenburg, C., Moridis, G., 1999. TOUGH2 User’s Guide, Version 2.0, Lawrence
627 Berkeley National Laboratory, Berkeley, CA.
628 Rutqvist, J., Tsang, C.F., 2003. Analysis of thermal-hydrologic-mechanical behavior near an
629 emplacement drift at Yucca Mountain, J Contam Hydrol 62-63, 637-652.
630 Rutqvist J., Börgesson L., Chijimatsu M., Nguyen T. S., Jing L., Noorishad J. and Tsang C.-F.
631 2001. Coupled Thermo-hydro-mechanical Analysis of a Heater Test in Fractured Rock
632 and Bentonite at Kamaishi Mine – Comparison of Field Results to Predictions of Four
633 Finite Element Codes. International Journal of Rock Mechanics and Mining Sciences,
634 38(1), 129-142.
635 Sacchi, E., Michelot, J.L., 2000. Porewater extraction from argillaceous rocks for geochemical
636 characterisation. Radiactive Waste Management. NEA, 185 pp.
637 Samper, J., Mon, A., Montenegro, L., 2018. A revisited thermal, hydrodynamic, chemical and
638 mechanical model of compacted bentonite for the entire duration of the FEBEX in situ
639 test. Applied Clay Science, 160: 58-70.
640 Samper, J., Zheng, L., Montenegro, L., Fernández, A.M., Rivas, P., 2008. Coupled thermo-
641 hydro-chemical models of compacted bentonite after FEBEX in situ test. Applied
642 Geochemistry, 23(5), 1186-1201.
643 Sánchez, M., Gens, A., Guimarães, L., 2012a. Thermal–hydraulic–mechanical (THM) behaviour
644 of a large-scale in situ heating experiment during cooling and dismantling. Canadian
645 Geotechnical Journal, 49(10), 1169-1195.
646 Sánchez, M., Gens, A., Guimarães, L.J.D.N., Olivella, S., 2005. A double structure generalized
647 plasticity model for expansive materials. International Journal for numerical and
648 analytical methods in geomechanics, 29: 751-787.
649 Sánchez, M., Gens, A., Olivella, S., 2012b. THM analysis of a large-scale heating test
650 incorporating material fabric changes. International Journal for Numerical and Analytical
651 Methods in Geomechanics, 36(4), 391-421.
652 Soler, J. M. 2001. The effect of coupled transport phenomena in the Opalinus Clay and
653 implications for radionuclide transport. Journal of Contaminant Hydrology 53: 63-84.

Tong, F., Jing, L., Zimmerman, R.W., 2010. A fully coupled thermo-hydro-mechanical model for simulating multiphase flow, deformation and heat transfer in buffer material and rock masses. International Journal of Rock Mechanics and Mining Sciences 47(2), 205-217.

Van Genuchten, M. T. 1980. A closed-form equation for predicting the hydraulic conductivity of unsaturated soils. Soil Science Society of America Journal 44(5), 892-898.

Villar, M.V. 2002. Thermo-hydro-mechanical characterisation of a bentonite from Cabo de Gata. A study applied to the use of bentonite as sealing material in high level radioactive waste repositories. Publicación Técnica ENRESA 01/2002, Madrid, 258 pp.

Villar, M.V., García-Siñeriz, J.L., Bárcena I., Lloret, A. 2005. State of the bentonite barrier after five years operation of an in situ test simulating a high level radioactive waste repository. Engineering Geology 80(3-4): 175-198.

Villar, M.V., Iglesias, R.J., Abós, H., Martínez, V., de la Rosa, C., Manchón, M.A. 2016. FEBEX-DP onsite analyses report. NAB 16-012. 106 pp.

Villar, M.V., Iglesias, R.J., Gutiérrez-Álvarez, C., Carbonell, B., 2018. Hydraulic and mechanical properties of compacted bentonite after 18 years in barrier conditions. Applied Clay Science 160, 49-57.

Xu, T., Sonnenthal, E., Spycher, N., Zheng, L., 2014. TOUGHREACT V3.0-OMP Reference Manual: A Parallel Simulation Program for Non-Isothermal Multiphase Geochemical Reactive Transport. Lawrence Berkeley National Laboratory, 2014.

Zheng, L., Samper, J., 2008. A coupled THMC model of FEBEX mock-up test. Physics and Chemistry of the Earth, Parts A/B/C, 33, Supplement 1: S486-S498.

Zheng, L., Samper, J., and Montenegro, L., 2008. Inverse hydrochemical models of aqueous extracts tests, Physics and Chemistry of the Earth, Parts A/B/C 33, 1009-1018.

Zheng, L., Samper, J., Montenegro, L., 2011. A coupled THC model of the FEBEX in situ test with bentonite swelling and chemical and thermal osmosis. Journal of Contaminant Hydrology, 126(1–2), 45-60.

Zheng, L., Samper, J., Montenegro, L., Fernández, A.M., 2010. A coupled THMC model of a heating and hydration laboratory experiment in unsaturated compacted FEBEX bentonite. Journal of Hydrology, 386(1–4), 80-94.

Zheng, L., Rutqvist, J., Birkholzer, J.T., Liu, H.H., 2015a. On the impact of temperatures up to 200 °C in clay repositories with bentonite engineer barrier systems: A study with coupled thermal, hydrological, chemical, and mechanical modeling. Engineering Geology 197, 278-295.

Zheng, L., Rutqvist, J., Kim, K., Houseworth, J., 2015b. Investigation of Coupled Processes and Impact of High Temperature Limits in Argillite Rock. FCRD-UFD-2015-000362, LBNL-187644.

Zheng, L., Kim, K., Xu, H., Rutqvist, J., 2016). DR Argillite Disposal R&D at LBNL. FCRD-UFD-2016-000437, LBNL-1006013.

Zheng, L., Rutqvist, J., Xu, H., Birkholzer, J.T., 2017. Coupled THMC models for bentonite in an argillite repository for nuclear waste: Illitization and its effect on swelling stress under high temperature. Engineering Geology 230, 118-129.

Zhou, Y., Rajapakse, R.K.N.D., Graham, J., 1999. Coupled Field in a deformable unsaturated medium. International Journal of Solid and Structures, 36, 4841-4868.

Table 1. *Timeline of FEBEX in situ test (ENRESA, 2000; Bárcena et al., 2003; Garcia-Sineriz et al., 2016)* .

Event	**Date**	**Time (day)**	**Time (year)**
Commencement of heating	2/27/1997	0	0.0
Shutdown of Heater #1	2/28/2002	1827	5.0
#Sampling bentonite	5/2/2002	1930	5.3
Shutdown of Heater #2	4/24/2015	6630	18.1
$Sampling bentonite	7/3/2015	6700	18.3

the sampling work started on 4/2/2002 and progressed section by section (Bárcena et al., 2003), when section 28, 29 (from where data in this paper were used) were sampled, it is about 5/2/2002.

$this is the time when section 49 was sampled.

711

712 Table 2. Thermal and hydrodynamic parameters.

Parameter	**Granite**	**Bentonite**
Grain density [kg/m^3]	2700	2780
Porosity ϕ	0.01	0.41
Saturated permeability [m^2]	2.0×10^{-18}	2.15×10^{-21}
Relative permeability, k_{rl}	$k_{rl} = S$	$k_{rl} = S^3$
Van Genuchten $1/\alpha$ [1/Pa]	4.76×10^{-4}	1.1×10^{-8}
Van Genuchten m	0.7	0.45
Compressibility, β [1/Pa]	3.2×10^{-9}	5.0×10^{-8}
Thermal expansion coeff. [1/^{o}C]	1.0×10^{-5}	1.5×10^{-4}
Dry specific heat [J/kg-^{o}C]	793	1091
Thermal conductivity [W/m-^{o}C] dry/wet	3.2/3.3	0.47/1.15
Effective vapor diffusion coefficient (m^2/s)	7.03×10^{-5}	7.03×10^{-5}

713 Note: in the relative permeability function, S is water saturation

714

715 *Table 3. Direct and coupled flux and phenomena (Horseman and McEwe., 1996; Soler, 2001)*

Flux	Gradient		
	Hydraulic	Temperature	Chemical
liquid	Hydraulic flow Darcy's law	Thermo-osmosis	Chemical osmosis
Heat	Convective heat flow	Thermal conduction Fourier's law	Dufour effect
Solute	Hyperfiltration	Thermal diffusion or Soret effect	Diffusion Fick's law

716

717

718

719 *Table 4 list of simulations, with difference from the base THMC model marked in red fonts.*

Simulations	Permeability	porosity	Mechanical process	Cl transport	Thermal osmosis	Non-Darcy flow	Vapor diffusion
TH model	Constant, 2.15×10^{-21} m^2	Constant, 0.41	No	No	No	No	7.03×10^{-5} m^2/s
Non-Darcy TH model	Constant, 2.15×10^{-21} m^2	Constant, 0.41	No	No	No	Yes	7.03×10^{-5} m^2/s
Base THMC model	Eq. (3) with an initial permeability of 2.15×10^{-21} m^2	According to mechanical model	Yes, Equation (5)	yes	Yes	No	7.03×10^{-5} m^2/s
Run A	Eq. (7) with an initial permeability of 2.15×10^{-21} m^2	According to mechanical model	Yes, Equation (5)	yes	Yes	No	7.03×10^{-5} m^2/s
Run B	Eq. (3) with an initial permeability of 2.15×10^{-21} m^2	According to mechanical model	Yes, Equation (5)	yes	No	No	7.03×10^{-5} m^2/s
Run C	Eq. (3) with an initial permeability of 2.15×10^{-21} m^2	According to mechanical model	Yes, Equation (5)	yes	Yes	No	2×10^{-4} m^2/s
Run D	Eq. (3) with an initial permeability of 1.5×10^{-21} m^2	According to mechanical model	Yes, Equation (5)	yes	Yes	No	7.03×10^{-5} m^2/s

720

721

722

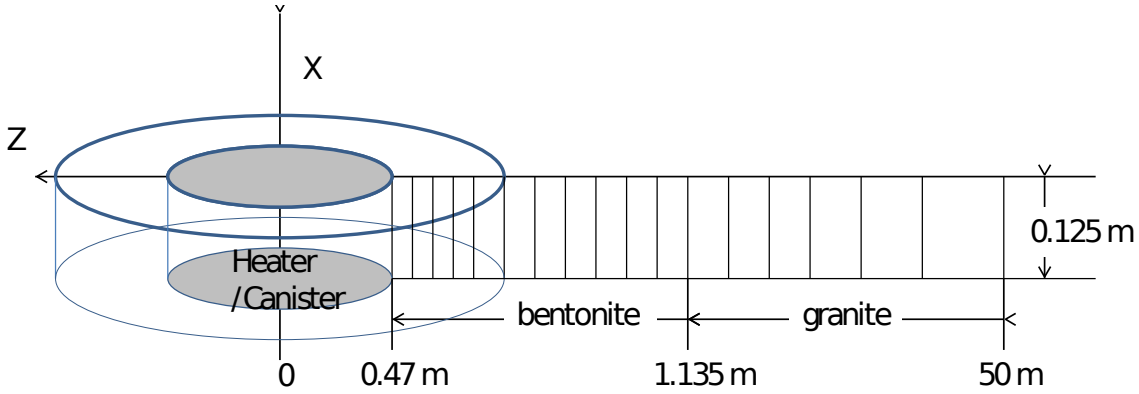

Fig. 1. Mesh used for the model, not to the scale.

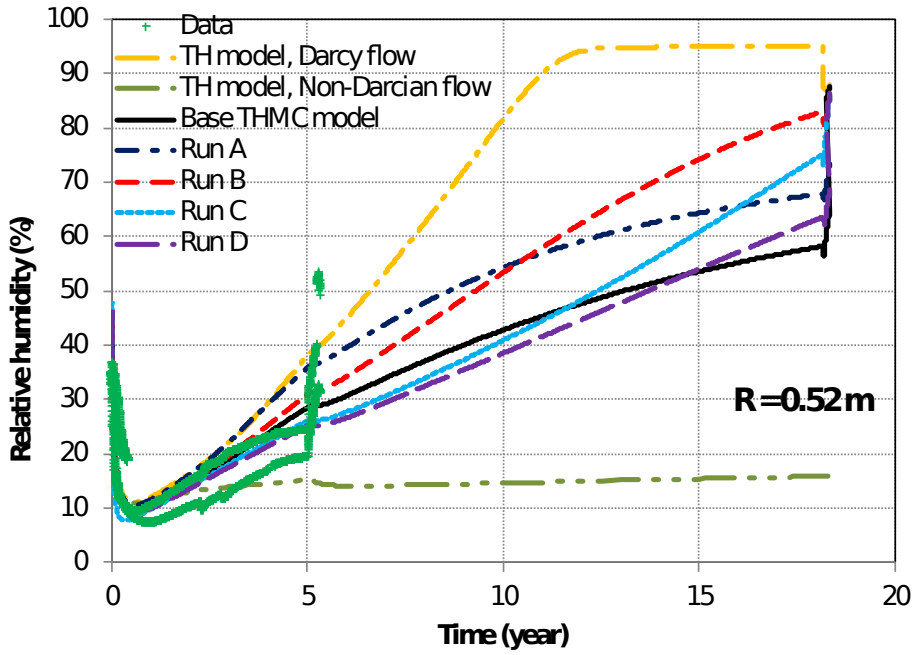

Fig. 2. Relative humidity data measured from sensors at different locations (from sections E1 and E2, see ENRESA(2006)) but the same radial distance (0.52 m) and model results from the base THMC model, Run A (similar to base THMC model but with different permeability function), Run B (thermal osmosis is disabled), Run C (similar to Run B but with higher vapor diffusion coefficient) and Run D (similar to Run B but with lower intrinsic permeability).

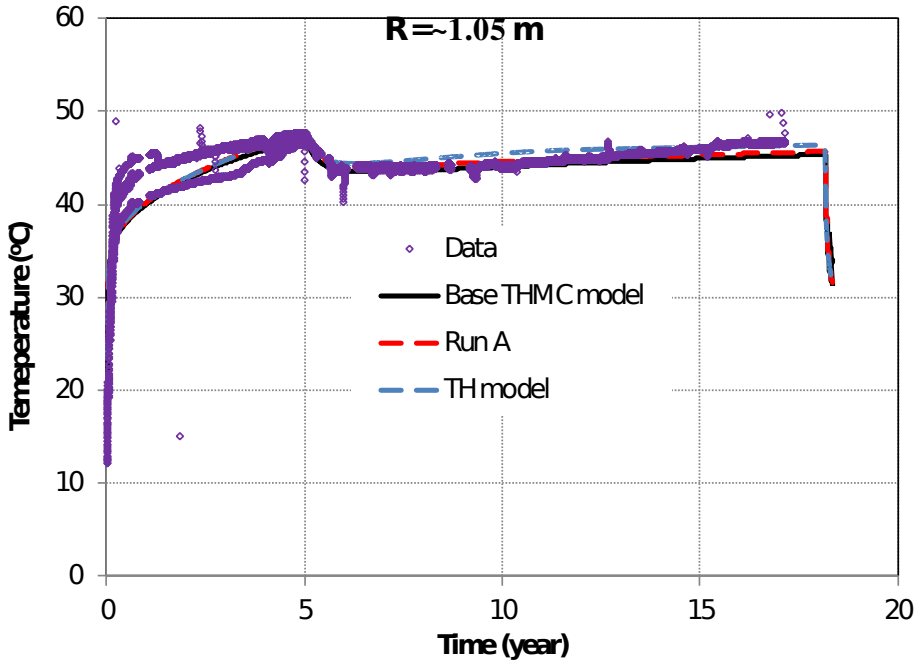

734

735 **Fig. 3.** Measured temperature by sensors at different locations (from section F2 and E2, see
736 ENRESA (2006)) but the same radial distance (1.05 m) and results from the TH model,
737 base THMC model and Run A (similar to base THMC model but with different permeability
738 function).
739

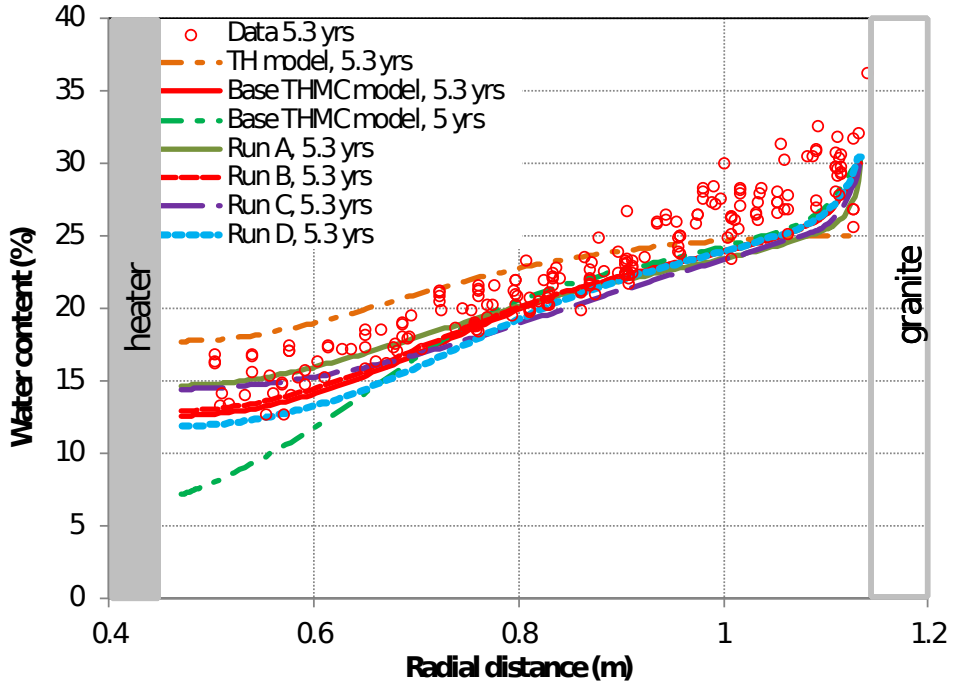

740

741

Fig. 4. Measured water content at 5.3 years (Villar et al. 2005), and results from the TH model, the base THMC model, Run A (similar to base THMC model but with different permeability function), Run B (thermal osmosis is disabled), Run C (similar to Run B but with higher vapor diffusion coefficient) and Run D (similar to Run B but with lower intrinsic permeability). Also shown are the model results from base THMC model at 5 years (before the cooling during the dismantling of heater #1).

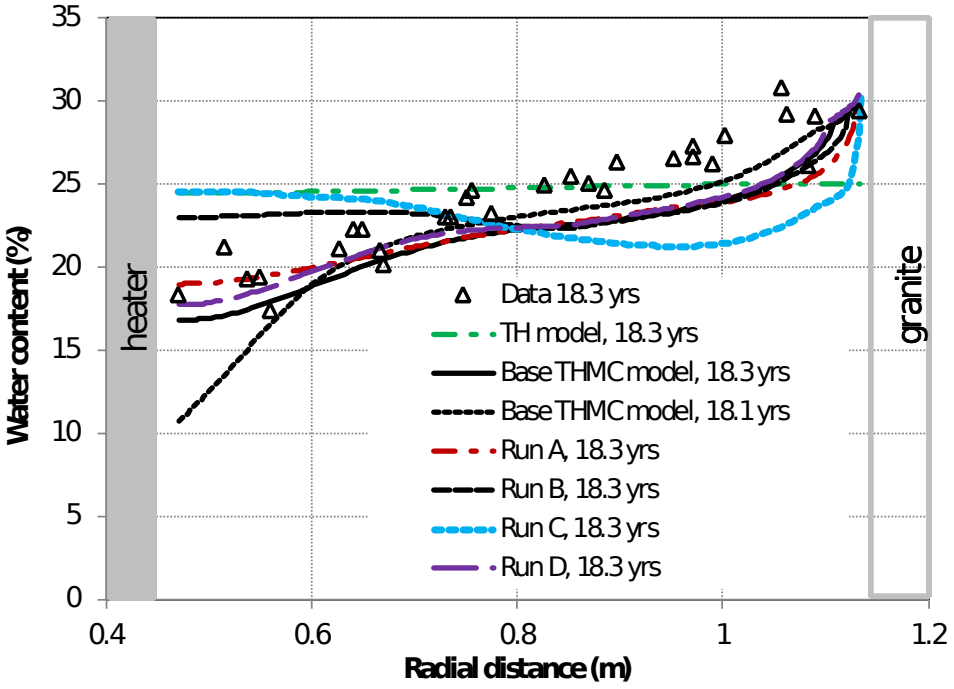

Fig. 5. Measured water content at 18.3 years (Villar et al. 2016), and results from the TH model, the base THMC model, Run A (similar to base THMC model but with different permeability function), Run B (thermal osmosis is disabled), Run C (similar to Run B but with higher vapor diffusion coefficient) and Run D (similar to Run B but with lower intrinsic permeability). Also shown are the model results from base THMC model at 18.1 years (before the cooling during the dismantling of heater #2).

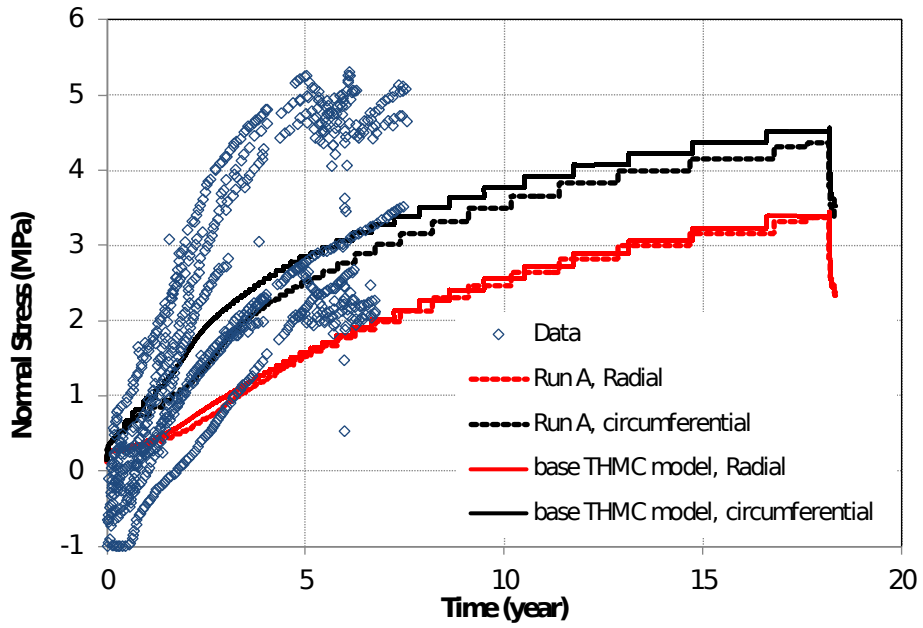

757

758 **Fig. 6.** Measured stress by sensors at different locations (from section E2 and F2, see ENRESA
759 (2000)) but the same radial distance (1.1 m) and results from the base THMC model and Run
760 A (similar to base THMC model but with different permeability function).
761

762

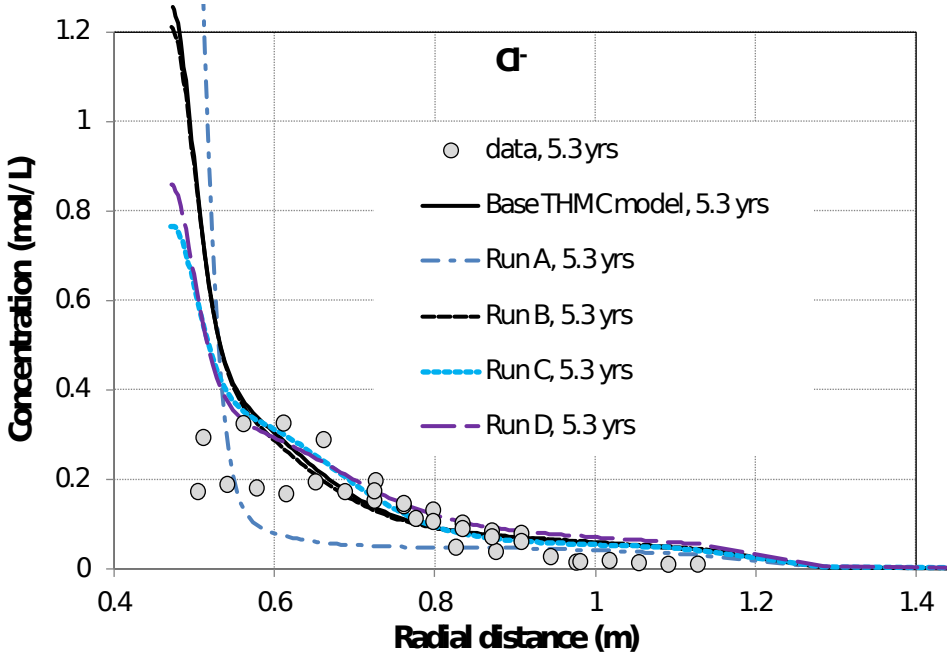

763

764 **Fig. 7.** Calibrated chloride concentration data at 5.3 years (Zheng et al., 2011) and model results
765 from the base THMC models, Run A (similar to base THMC model but with different
766 permeability function), Run B (thermal osmosis is disabled), Run C (similar to Run B but
767 with higher vapor diffusion coefficient) and Run D (similar to Run B but with lower intrinsic
768 permeability).
769

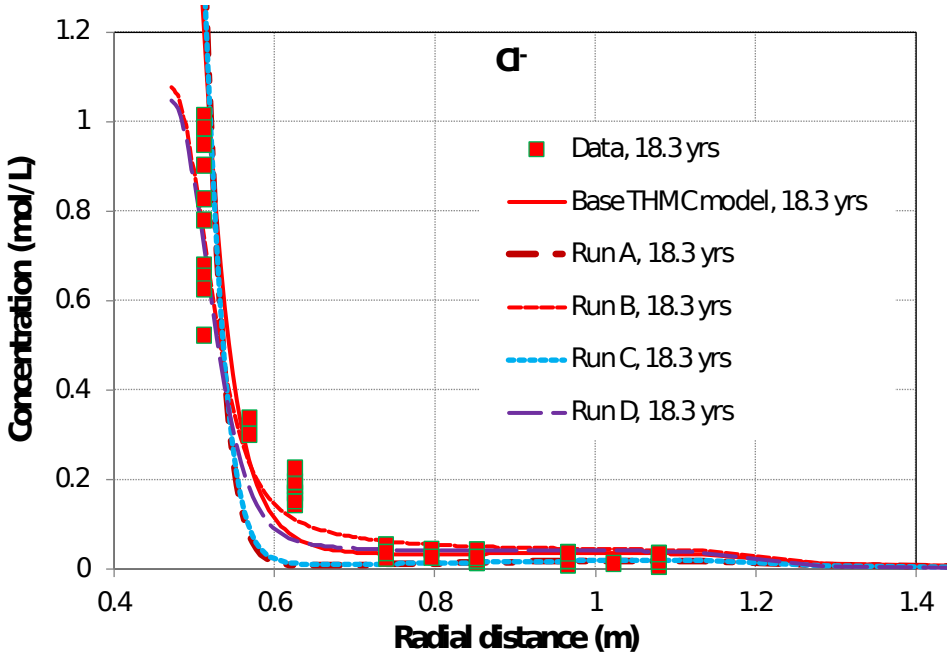

770

771 **Fig. 8.** Calibrated chloride concentration data at 18.3 years and model results from the base
772 THMC models, Run A (similar to base THMC model but with different permeability
773 function), Run B (thermal osmosis is disabled), Run C (similar to Run B but with higher
774 vapor diffusion coefficient) and Run D (similar to Run B but with lower intrinsic
775 permeability).
776

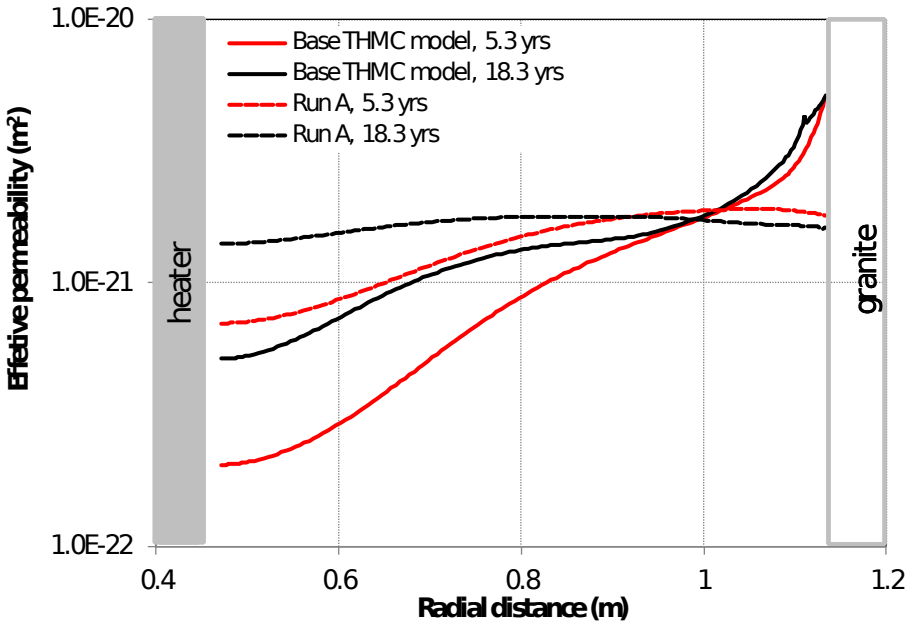

Fig. 9. Computed effective permeability (product of intrinsic permeability and relative permeability) at 5.3 and 18.3 years from the base THMC models and Run A (similar to base THMC model but with different permeability function).